

A POSTERIORI ERROR ANALYSIS AND AN ADAPTIVE STRATEGY FOR A GENERALIZED STOKES PROBLEM*

Rodolfo Araya *, Gabriel Barrenechea *, and Abner Poza *

*Departamento de Ingeniería Matemática
Universidad de Concepción
Casilla 160-C, Concepción, Chile
email: raraya, gbarrene, abner@ing-mat.udec.cl

Key Words: Stokes equation, a posteriori error estimator, bubble function, stabilized finite element method.

Abstract. *In this work we propose a new a posteriori error estimator for the Stokes problem, both with and without a reaction term. This hierarchical type estimator is based on the solution of local problems posed on appropriate finite dimensional spaces of bubble-like functions. An equivalence result between the norm of the finite element error and the estimator is given, where the dependence of the constants on the physics of the problem is explicated. Several numerical results confirming both the theoretical results and the good performance of the estimator are given.*

*The work of Rodolfo Araya and Abner Poza has been partially supported by CONICYT through FONDECYT Project No. 1040595. Gabriel Barrenechea has been partially supported by CONICYT through FONDECYT Project No. 1030674 and by FONDAP Program in Applied Mathematics.

1 INTRODUCTION

A posteriori error analysis in problems related to fluid dynamics is a subject to the one lot of attention has been paid in the last decades. For instance, for the advective-diffusive model we can quote the works¹⁻⁴ among others. Now, for the Stokes problem, the works by Verfürth^{5,6} and Bank and Welfert⁷ laid the basic foundation for the mathematical analysis of practical methods (see also⁸ for error estimators in the nonconforming case). More recently, in^{9,10} and¹¹ a posteriori error estimators rigorously bounding the discretization errors have been addressed. All previous references deal with stable (in the sense of the discrete inf-sup condition¹²) discretizations for the Stokes problem. In¹³ an a posteriori error analysis of stabilized formulations for the Stokes problem was performed.

In this work, we propose an a posteriori error estimator on the hierarchical type for a stabilized discretization of the Stokes problem, with and without reaction. Our approach is based on an idea from¹⁰ building an auxiliary problem, whose solution is equivalent with the norm of the finite element error. Since this auxiliary problem is posed on an infinite dimensional setting, we build a hierarchical estimation for the solution of this problem, which turns out to be equivalent with this solution, and hence the resulting finite element approximation is equivalent to the original finite element error.

An outline of the paper is as follows. The model problem is stated in Section 2. Next, in Section 3 we propose the auxiliary problem (with the discrete residual as right hand side) and prove a first equivalence result between the norm of the error and the solution of the auxiliary problem. As we told before, the auxiliary problem is posed on an infinite dimensional space, and hence in Section 4 we define a hierarchical a posteriori error estimator to approximate it. The development of this estimator needs a technical assumption on the local spaces to be used, and hence in Section 5 we propose a concrete set of local spaces satisfying this technical (LBB) condition. Finally, in Section 6 we give several numerical results confirming the theoretical results and showing the good performance of our estimator.

2 THE MODEL PROBLEM

Let $\Omega \subseteq \mathbb{R}^2$ a bounded open set with polygonal boundary Γ . We denote by $H^m(\Omega)$ the usual Sobolev space of order $m \geq 0$, with norm $\|\cdot\|_{m,\Omega}$ and seminorm $|\cdot|_{m,\Omega}$, respectively (with the convention $H^0(\Omega) = L^2(\Omega)$ and $|\cdot|_{0,\Omega} = \|\cdot\|_{0,\Omega}$). Then, given $\mathbf{f} \in L^2(\Omega)^2$, $\sigma \geq 0$ and $\nu \in \mathbb{R}^+$, our generalized Stokes problem reads: *Find* $(\mathbf{u}, p) \in H^1(\Omega)^2 \times L_0^2(\Omega)$ such that

$$(P) \begin{cases} \mathcal{L}(u, p) := \sigma \mathbf{u} - \nu \Delta \mathbf{u} + \nabla p = \mathbf{f} & \text{in } \Omega, \\ \operatorname{div} \mathbf{u} = 0 & \text{in } \Omega, \\ \mathbf{u} = \mathbf{0} & \text{on } \Gamma, \end{cases}$$

where $L_0^2(\Omega) := \{q \in L^2(\Omega) : (q, 1)_\Omega = 0\}$, where $(\cdot, \cdot)_D$ stands for the inner product in $L^2(D)$ (or in $L^2(D)^2$, $L^2(D)^{2 \times 2}$, if necessary). Let then $\mathbf{H} := H_0^1(\Omega)^2$ and $Q := L_0^2(\Omega)$ be the functional spaces to be used. The weak formulation of problem (P) reads: *Find* $(\mathbf{u}, p) \in \mathbf{H} \times Q$

such that

$$a(\mathbf{u}, \mathbf{v}) + b(\mathbf{v}, p) + b(\mathbf{u}, q) = F(\mathbf{v}, q) \quad \forall (\mathbf{v}, q) \in \mathbf{H} \times Q, \quad (1)$$

where

$$a(\mathbf{u}, \mathbf{v}) := \sigma(\mathbf{u}, \mathbf{v})_{\Omega} + \nu(\nabla \mathbf{u}, \nabla \mathbf{v})_{\Omega}, \quad (2)$$

$$b(\mathbf{v}, q) := -(q, \operatorname{div} \mathbf{v})_{\Omega}, \quad (3)$$

$$F(\mathbf{v}, q) := (\mathbf{f}, \mathbf{v})_{\Omega}.$$

In some places, we will write $a_D(\cdot, \cdot)$ to denote integration over $D \subseteq \mathbb{R}^2$. Furthermore, let $c : Q \times Q \rightarrow \mathbb{R}$ be the symmetric bilinear form defined by:

$$c(p, q) := \frac{1}{\nu} (p, q)_{\Omega}.$$

Using bilinear forms a and c we define the following norms:

$$\|\mathbf{v}\|_a := a(\mathbf{v}, \mathbf{v})^{1/2} \quad \forall \mathbf{v} \in \mathbf{H},$$

$$\|q\|_c := c(q, q)^{1/2} \quad \forall q \in Q,$$

and use them to define the following norm on the product space $\mathbf{H} \times Q$:

$$\|(\mathbf{v}, q)\| := \left\{ \|\mathbf{v}\|_a^2 + \|q\|_c^2 \right\}^{1/2} \quad \forall (\mathbf{v}, q) \in \mathbf{H} \times Q. \quad (4)$$

Using the classical theory of Babuska-Brezzi (cf.¹⁴) we can state the following result.

Lemma 1 *Weak problem (1) has a unique solution $(\mathbf{u}, p) \in \mathbf{H} \times Q$.*

3 THE AUXILIARY PROBLEM AND THE RESIDUAL EQUATION

We start by giving some notations that will be useful in the sequel. First, let $\{\mathcal{T}_h\}_{h>0}$ be a regular family of triangulations of Ω and let us denote by \mathcal{E}_h the set of all sides of \mathcal{T}_h with the usual splitting $\mathcal{E}_h = \mathcal{E}_{\Omega} \cup \mathcal{E}_{\Gamma}$, where \mathcal{E}_{Ω} stand for the sides lying on the interior of Ω . Also, for $T \in \mathcal{T}_h$, we denote by $\mathcal{N}(T)$ the set of nodes of T and by $\mathcal{E}(T)$ the set of sides of T . Also, for $F \in \mathcal{E}_h$ we define the following neighborhood:

$$\omega_F := \bigcup_{F \in \mathcal{E}(T')} T'.$$

Next, for $T \in \mathcal{T}_h$ and $F \in \mathcal{E}_{\Omega}$, let h_T be the diameter of T , $h_F := |F|$.

In the rest of the paper we will use the notation

$$a \preceq b \iff a \leq K b,$$

$$a \simeq b \iff a \preceq b \text{ and } b \preceq a,$$

where the positive constant K is independent of h, σ and ν .

Finally, we introduce the following finite element spaces

$$\begin{aligned} \mathbf{H}_h &:= \{\varphi \in C(\bar{\Omega})^2 : \varphi|_T \in \mathbb{P}_1(T)^2, \forall T \in \mathcal{T}_h\} \cap H_0^1(\Omega)^2, \\ Q_h &:= \{\varphi \in C(\bar{\Omega}) : \varphi|_T \in \mathbb{P}_1(T), \forall T \in \mathcal{T}_h\} \cap L_0^2(\Omega), \end{aligned}$$

and present the stabilized finite element method to be considered in this paper (cf.¹⁵): *Find* $(\mathbf{u}_h, p_h) \in \mathbf{H}_h \times Q_h$ *such that*:

$$A_\delta((\mathbf{u}_h, p_h), (\mathbf{v}_h, q_h)) = F_\delta(\mathbf{v}_h, q_h) \quad \forall (\mathbf{v}_h, q_h) \in \mathbf{H}_h \times Q_h, \quad (5)$$

where

$$\begin{aligned} A_\delta((\mathbf{u}_h, p_h), (\mathbf{v}_h, q_h)) &:= a(\mathbf{u}_h, \mathbf{v}_h) + b(\mathbf{v}_h, p_h) + b(\mathbf{u}_h, q_h) \\ &\quad - \sum_{T \in \mathcal{T}_h} \delta_T (\mathcal{L}(\mathbf{u}_h, p_h), \mathcal{L}(\mathbf{v}_h, q_h))_T, \end{aligned}$$

and

$$F_\delta(\mathbf{v}_h, q_h) := F(\mathbf{v}_h) - \sum_{T \in \mathcal{T}_h} \delta_T (\mathbf{f}, \mathcal{L}(\mathbf{v}_h, q_h))_T.$$

If $\sigma > 0$, stabilization parameter δ_T is given by:

$$\delta_T := \frac{h_T^2}{\sigma h_T^2 \max\{\lambda_T, 1\} + 12\nu}, \quad (6)$$

where

$$\lambda_T := \frac{12\nu}{\sigma h_T^2}.$$

If $\sigma = 0$, we recover the GLS method¹⁶ with $\delta_T = h_T^2/24\nu$.

The starting point in the construction of our a posteriori error estimator is the following auxiliary problem: *Find* (ϕ, ψ) *such that*:

$$a(\phi, \mathbf{v}) + c(\psi, q) = F(\mathbf{v}, q) - a(\mathbf{u}_h, \mathbf{v}) - b(\mathbf{v}, p_h) - b(\mathbf{u}_h, q), \quad (7)$$

for all (\mathbf{v}, q) in $\mathbf{H} \times Q$, or, written in another way

$$a(\phi, \mathbf{v}) + c(\psi, q) = \mathcal{R}_h(\mathbf{v}, q) \quad \forall (\mathbf{v}, q) \in \mathbf{H} \times Q, \quad (8)$$

where $\mathcal{R}_h : \mathbf{H} \times Q \rightarrow \mathbb{R}$ stands for the residual functional given by

$$\mathcal{R}_h(\mathbf{v}, q) := F(\mathbf{v}, q) - a(\mathbf{u}_h, \mathbf{v}) - b(\mathbf{v}, p_h) - b(\mathbf{u}_h, q).$$

This auxiliary problem is clearly uncoupled. Indeed, taking alternatively $\mathbf{v} = \mathbf{0}$ and $q = 0$ in (8) we have

$$a(\phi, \mathbf{v}) = (\mathbf{f}, \mathbf{v})_\Omega - a(\mathbf{u}_h, \mathbf{v}) - b(\mathbf{v}, p_h) =: \mathcal{R}_h^1(\mathbf{v}) \quad \forall \mathbf{v} \in \mathbf{H}, \quad (9)$$

$$c(\psi, q) = -b(\mathbf{u}_h, q) \quad \forall q \in Q. \quad (10)$$

Remark 2 From (10) we have

$$\int_{\Omega} (\nu^{-1}\psi - \operatorname{div} \mathbf{u}_h) q \, dx = 0 \quad \forall q \in Q,$$

and hence, since $\nu^{-1}\psi - \operatorname{div} \mathbf{u}_h \in Q$, we can see that

$$\psi = \nu \operatorname{div} \mathbf{u}_h,$$

from where we have an explicit solution for ψ .

In order to give a more precise (and useful in the sequel) expression for \mathcal{R}_h^1 , denoting $\boldsymbol{\varepsilon}_h := \nu \nabla \mathbf{u}_h - p_h \mathbf{I}$ (where \mathbf{I} stands for the $\mathbb{R}^{2 \times 2}$ identity matrix), integration by parts leads to

$$\mathcal{R}_h^1(\mathbf{v}) = \sum_{T \in \mathcal{T}_h} (\mathbf{R}_T, \mathbf{v})_T + \sum_{F \in \mathcal{E}_\Omega} (\mathbf{R}_F, \mathbf{v})_F, \quad (11)$$

where $\mathbf{R}_T \in L^2(T)^2$ and $\mathbf{R}_F \in L^2(F)^2$ are given by

$$\mathbf{R}_T := (\mathbf{f} - \mathcal{L}(\mathbf{u}_h, p_h))|_T,$$

and

$$\mathbf{R}_F := - [\boldsymbol{\varepsilon}_h \cdot \mathbf{n}]_F,$$

where $[[v]]_F$ stands for the jump of v across F .

We state now the following equivalence result.

Theorem 3 Let \mathbf{e} and E be the errors in approximating the velocity and pressure, respectively, i.e.

$$\mathbf{e} := \mathbf{u} - \mathbf{u}_h \quad , \quad E := p - p_h.$$

Then, the following equivalence result holds

$$\|\boldsymbol{\phi}\|_a^2 + \nu \|\operatorname{div} \mathbf{u}_h\|_{0,\Omega}^2 \preceq \|\mathbf{e}\|_a^2 + \|E\|_c^2 \preceq \left(\frac{\sigma + \nu}{\nu} \right)^2 \left[\|\boldsymbol{\phi}\|_a^2 + \nu \|\operatorname{div} \mathbf{u}_h\|_{0,\Omega}^2 \right],$$

where the equivalence constants are independent of h, σ and ν .

Proof. The proof follows from the properties of the bilinear forms a and c and the fact that $\psi = \nu \operatorname{div} \mathbf{u}_h$. For details, see¹⁷ Sections 3 and 4. \square

Based on this result in next section we will build an a posteriori error estimator for $\boldsymbol{\phi}$.

4 THE HIERARCHICAL ERROR ESTIMATOR

Let W_h be a finite element space such that

$$W_h = H_h + \sum_{T \in \mathcal{T}_h} \mathbf{H}_T^b + \sum_{F \in \mathcal{E}_\Omega} \mathbf{H}_F^b,$$

where $\mathbf{H}_T^b \subset H_0^1(T)^2$ and $\mathbf{H}_F^b \subset H_0^1(\omega_F)^2$ are finite dimensional spaces called *bubble subspaces*.

Using these notations we define our *hierarchical a posteriori error estimator* η_H by

$$\eta_H = \left\{ \sum_{T \in \mathcal{T}_h} a(P_T \phi, P_T \phi) + \sum_{F \in \mathcal{E}_\Omega} a(P_F \phi, P_F \phi) \right\}^{1/2}, \quad (12)$$

where ϕ is the solution of (9) and, for $S = T$ or $S = F$, $P_S \phi$ is the solution of the local problem: Find $P_S \phi \in \mathbf{H}_S^b$ such that

$$a(P_S \phi, \mathbf{v}_S) = \mathcal{R}_h^1(\mathbf{v}_S) \quad \forall \mathbf{v}_S \in \mathbf{H}_S^b.$$

Finally, we will suppose that the bubble subspaces satisfy the following inf–sup condition (LBB): There exists $\beta > 0$, independent of h, σ and ν , such that

$$\begin{aligned} \sup_{\mathcal{B}_T \in \mathbf{H}_T^b} \frac{(\mathcal{B}_T, \mathbf{R}_T)_T}{a_T(\mathcal{B}_T, \mathcal{B}_T)^{1/2}} &\geq \beta \theta_T \|\mathbf{R}_T\|_{0,T} & \forall T \in \mathcal{T}_h, \\ \sup_{\mathcal{B}_F \in \mathbf{H}_F^b} \frac{(\mathcal{B}_F, \mathbf{R}_F)_F}{a_{\omega_F}(\mathcal{B}_F, \mathcal{B}_F)^{1/2}} &\geq \beta \theta_F \|\mathbf{R}_F\|_{0,F} & \forall F \in \mathcal{E}_\Omega, \end{aligned}$$

where θ_T and θ_F are the mesh dependent constants given by

$$\begin{aligned} \theta_T &:= \begin{cases} \nu^{-1/2} h_T & , \quad \sigma = 0, \\ \sigma^{-1/2} \min\{h_T \sigma^{1/2} \nu^{-1/2}, 1\} & , \quad \sigma > 0. \end{cases} \\ \theta_F &:= \begin{cases} \nu^{-1/2} h_F^{1/2} & , \quad \sigma = 0, \\ \nu^{-1/4} \sigma^{-1/4} \min\{h_F \sigma^{1/2} \nu^{-1/2}, 1\}^{1/2} & , \quad \sigma > 0. \end{cases} \end{aligned}$$

Remark 4 In Section 5, we will give a concrete example of bubble function spaces satisfying (LBB).

Under the (LBB) assumption, and using some particular features of the stabilized finite element method (5), we can state the following equivalence result, whose proof may be found in¹⁷ Theorem 11.

Theorem 5 Let ϕ be the solution of (9). If (LBB) holds, then

$$a(\phi, \phi) \simeq \eta_H^2,$$

where η_H is given by (12) and the equivalence constants are independent of h, σ and ν .

Finally, from Theorems 3 and 5, we can state the following main result.

Theorem 6 Let (\mathbf{u}, p) , (\mathbf{u}_h, p_h) and ϕ be the solutions of (1), (5) and (9), respectively. If (LBB) holds, then the following equivalence holds

$$\sum_{T \in \mathcal{T}_h} \tilde{\eta}_{H,T}^2 \preceq \|\mathbf{u} - \mathbf{u}_h\|_a^2 + \|p - p_h\|_c^2 \preceq \left(\frac{\sigma + \nu}{\nu} \right)^2 \sum_{T \in \mathcal{T}_h} \tilde{\eta}_{H,T}^2,$$

where

$$\tilde{\eta}_{H,T} := \left\{ a(P_T \phi, P_T \phi) + \frac{1}{2} \sum_{F \in \mathcal{E}(T) \cap \mathcal{E}_\Omega} a(P_F \phi, P_F \phi) + \nu \|\operatorname{div} \mathbf{u}_h\|_{0,T}^2 \right\}^{1/2}.$$

5 BUBBLE FUNCTION SPACES SATISFYING (LBB) CONDITION

For each element $T \in \mathcal{T}_h$ we define the *element bubble function* b_T by

$$b_T := 27 \prod_{x \in \mathcal{N}(T)} \lambda_x, \tag{13}$$

where λ_x denotes the barycentric coordinate associated to node x . Following Verfürth¹ let \hat{T} be the standard reference element, of vertices $(1, 0)$, $(0, 1)$ and $(0, 0)$. Given any number $\alpha \in (0, 1]$ denote by $\Phi_\alpha : \mathbb{R}^2 \rightarrow \mathbb{R}^2$ the transformation which maps (x, y) onto $(x, \alpha y)$. Let

$$\hat{T}_\alpha := \Phi_\alpha(\hat{T}),$$

and denote by $\hat{\lambda}_{1,\alpha}$, $\hat{\lambda}_{2,\alpha}$ and $\hat{\lambda}_{3,\alpha}$ its barycentric coordinates (see Figure 1).

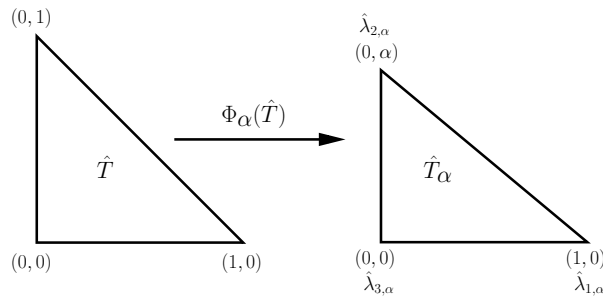


Figure 1: Triangles \hat{T} and \hat{T}_α .

Set

$$b_{\hat{F},\alpha} := \begin{cases} 4\hat{\lambda}_{3,\alpha}\hat{\lambda}_{1,\alpha} & \text{on } \hat{T}_\alpha, \\ 0 & \text{on } \hat{T} \setminus \hat{T}_\alpha, \end{cases}$$

where $\hat{F} := \{(t, 0) \in \mathbb{R}^2 : 0 \leq t \leq 1\}$. Let $F \in \mathcal{E}_\Omega$ and denote by T_1, T_2 two triangles which have F in common. Denote by $G_{F,i}$, $i = 1, 2$, the orientation preserving affine transformation which maps \hat{T} onto T_i and \hat{F} onto F (see Figure 2).

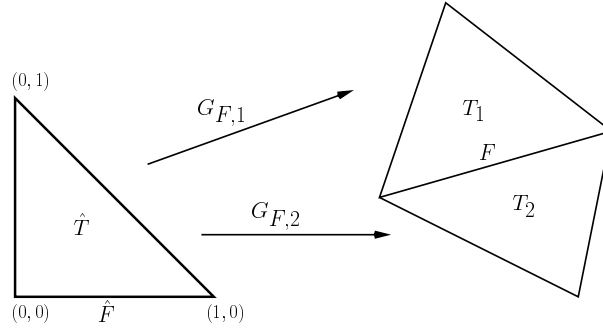


Figure 2: Affine transformation $G_{F,i}$, $i = 1, 2$.

Set

$$b_{F,\alpha} := \begin{cases} b_{\hat{F},\alpha} \circ G_{F,i}^{-1} & \text{on } T_i, i = 1, 2, \\ 0 & \text{on } \Omega \setminus \omega_F. \end{cases} \quad (14)$$

Let $\hat{\Pi} := \{(x, 0) : x \in \mathbb{R}\}$ and let $\hat{Q} : \mathbb{R}^2 \rightarrow \hat{\Pi}$ the orthogonal projection from \mathbb{R}^2 to $\hat{\Pi}$. We introduce the lifting operator $\hat{P}_{\hat{F}} : \mathbb{P}_k(\hat{F}) \rightarrow \mathbb{P}_k(\hat{T})$ by

$$\hat{P}_{\hat{F}}(\hat{s}) = \hat{s} \circ \hat{Q}.$$

Let $T_i \subseteq \omega_F$ and let $G_{F,i}$ the affine transformation defined in Figure 2. We define the lifting operator $P_{F,T_i} : \mathbb{P}_k(F) \rightarrow \mathbb{P}_k(T_i)$ by

$$P_{F,T_i}(s) = \hat{P}_{\hat{F}}(s \circ G_{F,i}) \circ G_{F,i}^{-1}.$$

Using these notations, we can define a lifting operator

$$s \in \mathbb{P}_k(F) \longrightarrow P_F(s) := \begin{cases} P_{F,T_1}(s) & \text{in } T_1, \\ P_{F,T_2}(s) & \text{in } T_2, \end{cases}$$

and, for $\mathbf{s} = (s_1, s_2) \in \mathbb{P}_k(F)^2$, we denote

$$\mathbf{P}_F(\mathbf{s}) = (P_F(s_1), P_F(s_2)).$$

Finally, for all $F \in \mathcal{E}_\Omega$ let α_F be the positive parameter given by

$$\alpha_F := \begin{cases} \min\{\nu^{1/2} \sigma^{-1/2} h_F^{-1}, 1\} & , \sigma > 0, \\ 1 & , \sigma = 0. \end{cases}$$

In order to satisfy (LBB) condition we need to impose the following condition on \mathbf{f} :
(F) \mathbf{f} is a piecewise polynomial function.

Next, we define the following bubble function spaces:

$$\begin{aligned} \mathbf{H}_T^b & := \langle \{b_T \mathbf{R}_T\} \rangle \quad \forall T \in \mathcal{T}_h, \\ \mathbf{H}_F^b & := \langle \{b_{F,\alpha_F} \mathbf{P}_F(\mathbf{R}_F)\} \rangle \quad \forall F \in \mathcal{E}_\Omega, \end{aligned}$$

where b_T and b_{F,α_F} are the bubble functions given by (13) and (14), respectively. It can be proved (see¹⁷) that the subspaces \mathbf{H}_T^b and \mathbf{H}_F^b defined above satisfy the (LBB) condition.

6 NUMERICAL RESULTS

In this section we report some results obtained for the standard Stokes problem (i.e. $\sigma = 0$), and the generalized one ($\sigma \neq 0$). In both cases we show the ability of an adaptive scheme, based on our a posteriori error estimator, to generate adapted meshes and to improve the discrete solution without using a highly refined uniform mesh.

6.1 The Stokes problem ($\sigma = 0$)

We present three sets of numerical experiments to validate our error estimator. From now on d.o.f. will denote the degrees of freedom associated with a particular mesh.

6.1.1 An analytical solution

For this test case, the domain is taken as the square $\Omega = (0, 1) \times (0, 1)$, $\nu = 1$, and \mathbf{f} is set such as the exact solution of our Stokes problem is given by

$$\begin{aligned} u_1(x, y) & = -256x^2(x-1)^2y(y-1)(2y-1), \\ u_2(x, y) & = -u_1(y, x), \\ p(x, y) & = 150(x-0.5)(y-0.5). \end{aligned}$$

In order to test our a posteriori error estimator in Figure 3 we depict the error, in the norm defined in (4), and estimator $\tilde{\eta}_H$ as $h \rightarrow 0$ using a sequence of uniformly refined meshes. We can observe that both values are in good accordance, which is confirmed in Table 1 where we show the effectivity index

$$E_i := \frac{\tilde{\eta}_H}{\|(\mathbf{u} - \mathbf{u}_h, p - p_h)\|},$$

which remains bounded as $h \rightarrow 0$. Finally, in order to study the sensitivity of effectivity index as $\nu \rightarrow 0$, we present in Table 2 the behavior of $\tilde{\eta}_H$ and $\|(\mathbf{u} - \mathbf{u}_h, p - p_h)\|$ for a fixed mesh and for $\nu = 1, 10^{-1}, \dots, 10^{-6}$. We observe that, as was predicted by Theorem 6, estimator $\tilde{\eta}_H$ follows the same pattern of $\|(\mathbf{u} - \mathbf{u}_h, p - p_h)\|$, and hence, the effectivity index remains bounded independently of the value of ν .

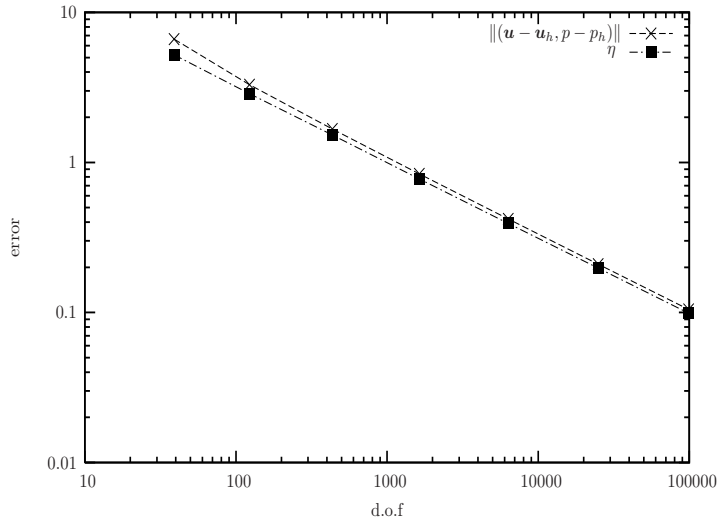


Figure 3: Exact error and the a posteriori error estimate.

| d.o.f | $\ (\mathbf{u} - \mathbf{u}_h, p - p_h)\ $ | $\tilde{\eta}_H$ | E_i |
|-------|--|------------------|----------|
| 39 | 6.641955 | 5.216376 | 0.785367 |
| 123 | 3.292848 | 2.873238 | 0.872569 |
| 435 | 1.671618 | 1.523188 | 0.911205 |
| 1635 | 0.838908 | 0.775193 | 0.924050 |
| 6339 | 0.419710 | 0.392412 | 0.934960 |
| 24963 | 0.209854 | 0.197351 | 0.940422 |
| 99075 | 0.104919 | 9.900770e-02 | 0.943655 |

Table 1: Exact error, a posteriori error estimator and effectivity index.

| ν | $\ (\mathbf{u} - \mathbf{u}_h, p - p_h)\ $ | $\tilde{\eta}_H$ | E_i |
|-------|--|------------------|----------|
| 1 | 0.209854 | 0.197351 | 0.940422 |
| 1e-01 | 6.643132e-02 | 6.244997e-02 | 0.940068 |
| 1e-02 | 2.309899e-02 | 2.105384e-02 | 0.911461 |
| 1e-03 | 3.123896e-02 | 2.392909e-02 | 0.766001 |
| 1e-04 | 9.655438e-02 | 7.305909e-02 | 0.756662 |
| 1e-05 | 0.305260 | 0.227342 | 0.744750 |
| 1e-06 | 0.965315 | 0.645566 | 0.668762 |

Table 2: Sensibility of the estimator to ν .

6.1.2 The lid-driven cavity problem

For this case we use the same domain as in previous section, we set $\mathbf{f} = \mathbf{0}$, and the boundary conditions $\mathbf{u} = \mathbf{0}$ on $[\{0\} \times (0, 1)] \cup [(0, 1) \times \{0\}] \cup [\{1\} \times (0, 1)]$ and $\mathbf{u} = (1, 0)^t$ on $(0, 1) \times \{1\}$. We show in Figure 4 the initial mesh and the adapted one obtained using our error estimate. In Figure 5 we depict the discrete pressure field obtained using the initial and adapted meshes where we note the improvement in the quality of the computed solution since the singular nature of the pressure is better captured in the adapted mesh.

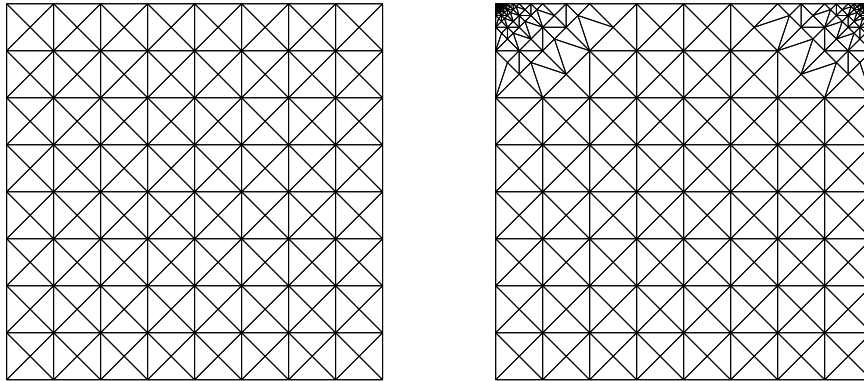


Figure 4: Initial and adapted meshes.

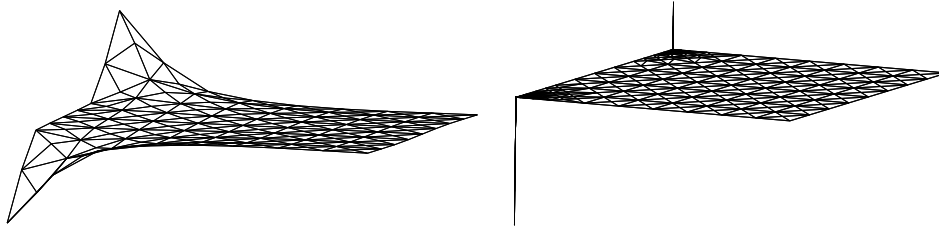


Figure 5: The pressure in the initial and adapted meshes.

6.1.3 The backward facing step problem

This test case is posed on the backward facing step configuration. The step is located at $(x, y) = (2.5, 0)$, the entry of the channel is at $x = 0$ and the exit of the channel at $x = 22$. The channel width is 1 at entry and 2 at exit. The boundary conditions are inflow parabolic profiles and free outflow. We assume $\mathbf{f} = \mathbf{0}$. In this case a singularity arises at the step from the re-entrant corner. Hence we can expect the meshes to be locally refined around the corner. In Figure 6 we depict the initial mesh, and in Figure 7 we show a zoom of the adapted mesh where we can observe the local behavior of the adapted mesh. Isovalues of the vertical component of the velocity are depicted in Figure 8 for both meshes. We remark the improvement in the quality of the discrete solution if we use the adapted mesh.

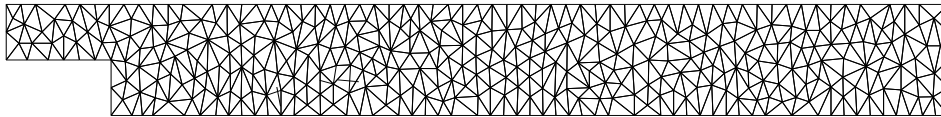


Figure 6: Initial mesh.

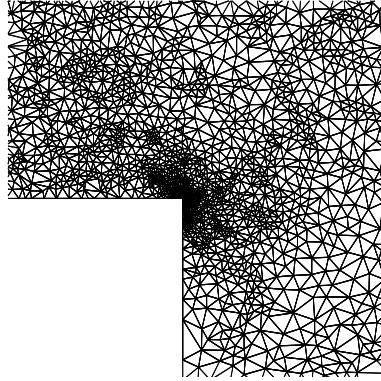


Figure 7: A zoom, near the singularity, of the adapted mesh.

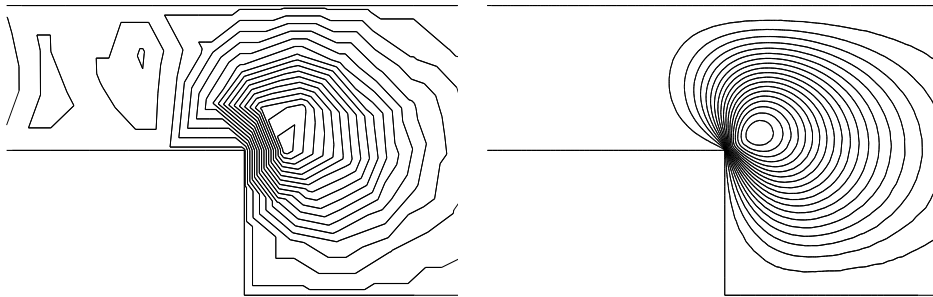


Figure 8: A zoom, near the singularity, of the normal velocity in the initial and the adapted meshes.

6.2 The generalized problem ($\sigma \neq 0$)

6.2.1 An analytical solution

For this test case we use the same analytical solution from Section 6.1.1. In Figures 9 and 10 we present the behavior, when $\nu = 1$ and $\sigma = 1, 10^6$, of the true error and the error estimate when h goes to 0 using again a sequence of uniformly refined meshes. In Tables 3 and 4 we show the same kind of information plus the effectivity index. Note that the exact error is quite well approached by our a posteriori error estimate.

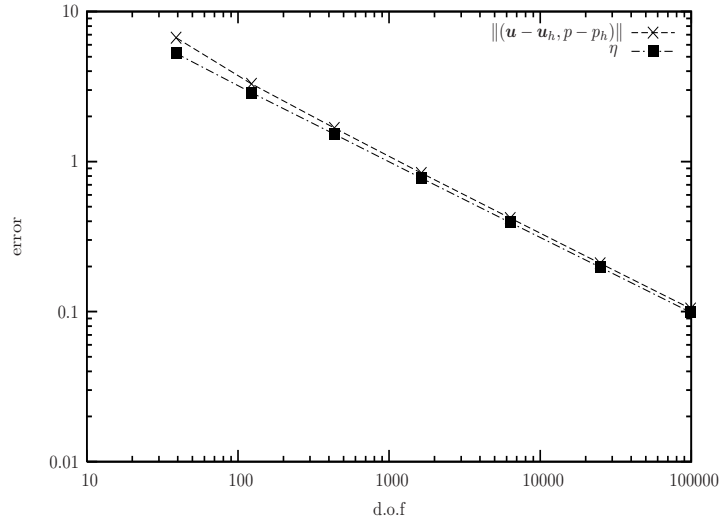


Figure 9: Exact error and the a posteriori error estimate ($\nu = 1$ and $\sigma = 1$).

| d.o.f | $\ (u - u_h, p - p_h)\ $ | η | E_i |
|-------|--------------------------|--------------|----------|
| 39 | 6.687539 | 5.263874 | 0.787116 |
| 123 | 3.298747 | 2.877562 | 0.872319 |
| 435 | 1.672377 | 1.523716 | 0.911107 |
| 1635 | 0.839004 | 0.775254 | 0.924016 |
| 6339 | 0.419722 | 0.392420 | 0.934951 |
| 24963 | 0.209856 | 0.197352 | 0.940419 |
| 99075 | 0.104919 | 9.900781e-02 | 0.943655 |

Table 3: Error, a posteriori error estimator and effectivity index ($\nu = 1$ and $\sigma = 1$).

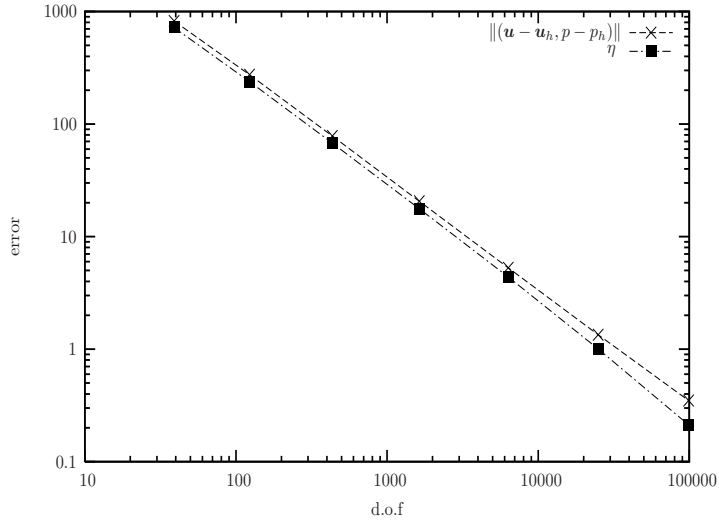


Figure 10: Exact error and the a posteriori error estimate ($\nu = 1$ and $\sigma = 10^6$).

| d.o.f | $\ (u - u_h, p - p_h)\ $ | η | E_i |
|-------|--------------------------|------------|----------|
| 39 | 821.888331 | 719.153888 | 0.875001 |
| 123 | 274.845840 | 238.693702 | 0.868463 |
| 435 | 78.294327 | 67.770544 | 0.865586 |
| 1635 | 20.622990 | 17.688430 | 0.857704 |
| 6339 | 5.2790531 | 4.381471 | 0.829972 |
| 24963 | 1.3445539 | 1.005010 | 0.747467 |
| 99075 | 0.3497008 | 0.212486 | 0.607624 |

Table 4: Error, a posteriori error estimator and effectivity index ($\nu = 1$ and $\sigma = 10^6$).

6.2.2 The lid-driven cavity problem

Again, we consider the problem described in Section 6.1.2, but in this case we assume $\nu = 1$ and $\sigma = 10^6$. In Figure 11 we depict the initial and final adapted meshes. We note that our a posteriori error estimate is able to detect correctly the boundary layer of the solution. In Figure 12 we show a vertical cross section of the first component of the velocity field. This cross section shows us the quality of the discrete solution computed using the adapted mesh. Note that the boundary layer is clearly captured.

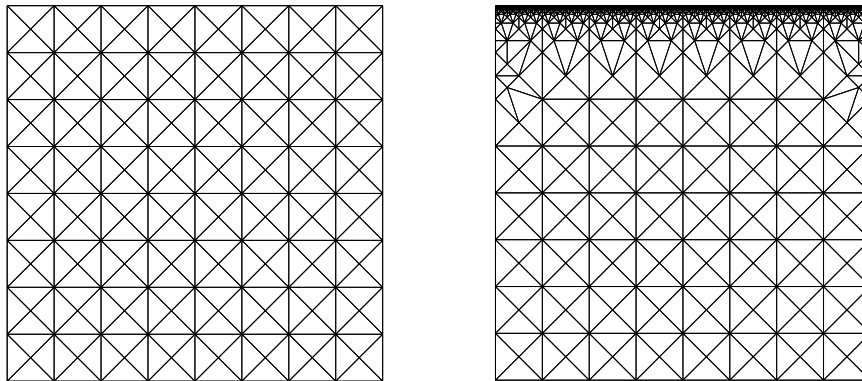


Figure 11: Initial and final adapted meshes.

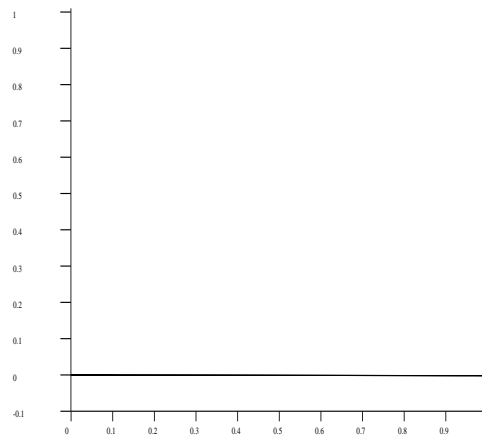


Figure 12: A cross section of the tangential velocity at $x = \frac{1}{2}$.

REFERENCES

- [1] R. Verfürth. A posteriori error estimators for convection-diffusion equations. *Numer. Math.*, **80**, 641–663 (1998).
- [2] V. John. A numerical study of a posteriori error estimators for convection-diffusion problems. *Comput. Methods Appl. Mech. Engrg.*, **190**, 757–781 (2000).
- [3] R. Araya, E. Behrens, and R. Rodríguez. An adaptive stabilized finite element scheme for the advection-reaction-diffusion equation. *Appl. Num. Math.*, **54**(3–4), 491–503 (2005).

- [4] R. Araya, A. Poza, and E.P. Stephan. A hierarchical a posteriori error estimate for an advection-diffusion-reaction problem. *Math. Models Methods Appl. Sci.*, **15**(7), 1119–1139 (2005).
- [5] R. Verfürth. A posteriori error estimators for the Stokes problem. *Numer. Math.*, **55**, 309–325 (1989).
- [6] R. Verfürth. A posteriori error estimators for the Stokes problem II. Non-conforming discretizations. *Numer. Math.*, **60**, 235–249 (1991).
- [7] R.E. Bank and B.D. Welfert. A posteriori error estimators for the Stokes problem. *SIAM J. Numer. Anal.*, **28**, 591–623 (1991).
- [8] E. Dari, R. Durán, and C. Padra. Error estimators for nonconforming finite element approximations of the Stokes problem. *Math. Comp.*, **64**, 1017–1033 (1995).
- [9] M. Ainsworth and J.T. Oden. A posteriori error estimators for the Stokes and Oseen equations. *SIAM J. Numer. Anal.*, **34**, 228–245 (1997).
- [10] M. Ainsworth and J.T. Oden. *A Posterior Error Estimation in Finite Element Analysis*. J. Wiley, (2000).
- [11] W. Dörfler and M. Ainsworth. Reliable a posteriori error control for non-conforming finite element approximation of Stokes flow. *Math. Comp.*, (2005).
- [12] F. Brezzi and M. Fortin. *Mixed and Hybrid Finite Element Methods*. Springer-Verlag, (1991).
- [13] D. Kay and D. Silvester. A posteriori error estimation for stabilized mixed approximations of the Stokes equations. *SIAM J. Scientific Computing*, **21**, 1321–1336 (1999).
- [14] V. Girault and P.A. Raviart. *Finite Element Methods for the Navier-Stokes Equations*. Springer-Verlag, (1986).
- [15] G. Barrenechea and F. Valentin. An unusual stabilized finite element method for a generalized Stokes problem. *Numer. Math.*, **92**(4), 653–677 (2002).
- [16] T.J.R. Hughes and L.P. Franca. A new finite element formulation for computational fluid dynamics: VII. The Stokes problem with various well-posed boundary conditions: Symmetric formulations that converge for all velocity/pressure spaces. *Comput. Methods Appl. Mech. Engrg.*, **65**(1), 85–96 (1987).
- [17] R. Araya, G. Barrenechea, and A. Poza. An a posteriori error estimator for the generalized stokes problem. Technical Report 2005-09, Departamento de Ingeniería Matemática, Universidad de Concepción, (2005).